ELSEVIER

Solid State Ionics 131 (2000) 61–68

SOLID STATE IONICS

www.elsevier.com/locate/ssi

Self-assembling nanostructures and atomic layer precise etching in molecular beam epitaxy

K. Eberl*, M.K. Zundel, H. Schuler

Max-Planck-Institut für Festkörperforschung, Heisenbergstrasse 1, 70569 Stuttgart, Germany

Received 24 November 1998; received in revised form 10 February 1999; accepted 15 February 1999

Abstract

We report on the preparation of 10 nm lateral size semiconductor structures based on island formation in strained layer growth in molecular beam epitaxy. Red light emitting InP quantum dot injection lasers are presented. They contain densely stacked layers of self-assembled InP quantum dots embedded in a $Ga_{0.51}In_{0.49}P$ wave guide layer. In the second part of this contribution we report on a new atomic layer precise etching technique in MBE, which allows improved interface control for the preparation of semiconductor nanostructures. The etching process involves $AsBr_3$ exposure of a GaAs or AlGaAs surface. Switching between atomic layer precise growth and etching is possible within a few seconds. © 2000 Elsevier Science B.V. All rights reserved.

Keywords: Molecular beam epitaxy; P-compounds; Self assembling quantum dots; Laser diodes; In-situ etching; Surface patterning; V-groove; MBE regrowth

PACS: 81.15.Hi; 78.66.Fd; 85.30.Vw; 42.55.Px

1. Introduction

Molecular beam epitaxy (MBE) allows atomic layer precise layer thickness control in semiconductor thin film deposition. Thin epitaxial layers are prepared by MBE for fast transistors and laser diodes in industrial production systems. The synthesis of lateral nanostructures is more difficult and generally involves lithography and etching in semiconductor technology which faces problems like limited resolution and defect introduction at the sidewalls due to reactive ion etching.

Extremely small 10 nm size quantum dots (QD) turned just recently out to be relatively easy to prepare by applying Stranski–Krastanow growth mode in strained layer heteroepitaxy [1]. Interesting applications for self-assembled QD in different material systems are light-emitting diodes and semiconductor laser diodes. Optoelectronic devices with QD on Si substrate are interesting due to the strong lateral localization of carriers in the active medium and the resulting reduced sensitivity to non-radiative recombination in threading dislocations, which are generally formed by growth of strain relaxed GaAs on Si substrate. Gerárd et al. reported about self

*Corresponding author. Tel.: +49-711-689-1312; fax: +49-711-689-1010.

E-mail address: eberl@servix.mpi-stuttgart.mpg.de (K. Eberl)

0167-2738/00/$ – see front matter
PII: S0167-2738(00)00622-6

assembled InAs dots in thick GaAs layers grown on Si which show improved photoluminescence (PL) as compared to layers with quantum wells [2]. For semiconductor lasers containing QD a lower threshold current density, a higher characteristic temperature, and an increased gain and differential gain in comparison with quantum well lasers were theoretically predicted [3,4] due to the discrete energy levels in zero-dimensional systems. For InAs [5] and $In_xGa_{1-x}As$ [6,7] dots in GaAs, and $In_xAl_{1-x}As$ in $Al_yGa_{1-y}As$ [8], injection lasers have been successfully demonstrated and show some of the characteristic properties which have been predicted.

Another currently more and more intensively investigated field is in-situ surface treatment. In the second part of this contribution we report about atomic layer precise etching in MBE with $AsBr_3$ as the etching species. Selective etching of SiO_2 masked GaAs (100) substrates allows in-situ preparation of extremely sharp V-grooves with almost perfectly planar {110} side facets. This new technique may become important in future for the preparation of monolithically integrated devices which involve two epitaxial growth steps with extensive processing in between.

2. Self assembling InP quantum dots

$Ga_{0.52}In_{0.48}P$ is lattice matched to GaAs substrate and has a direct band gap at 1.95 eV at 4 K. The lattice mismatch between InP and $Ga_{0.52}In_{0.48}P$ is 3.7%. The deposition of InP on a $Ga_{0.52}In_{0.48}P$ layer results in island formation after exceeding 1.5 monolayers. The size of the InP islands is about 15 nm in diameter and 2–3 nm in height after deposition of three monolayers of InP. The density is about 5×10^{10} cm^2 as shown in the atomic force micrograph in Fig. 1 [12]. These InP islands form almost ideal quantum dots because of their extremely small size and because they can be fully embedded in the barrier material $Ga_{0.52}In_{0.48}P$ by MBE overgrowth. Vertical stacking of layers with InP islands results in a strong correlation of the islands due to strain fields. The InP islands in the second and third layer tend to nucleate preferentially right above the underlayer islands if the spacer layer is thinner than the extension of the strain field [1].

A cross-sectional transmission electron micrograph (TEM) of the QD laser structure is shown in Fig. 2. The growth and fabrication details are presented elsewhere [9]. The InP dots appear as dark

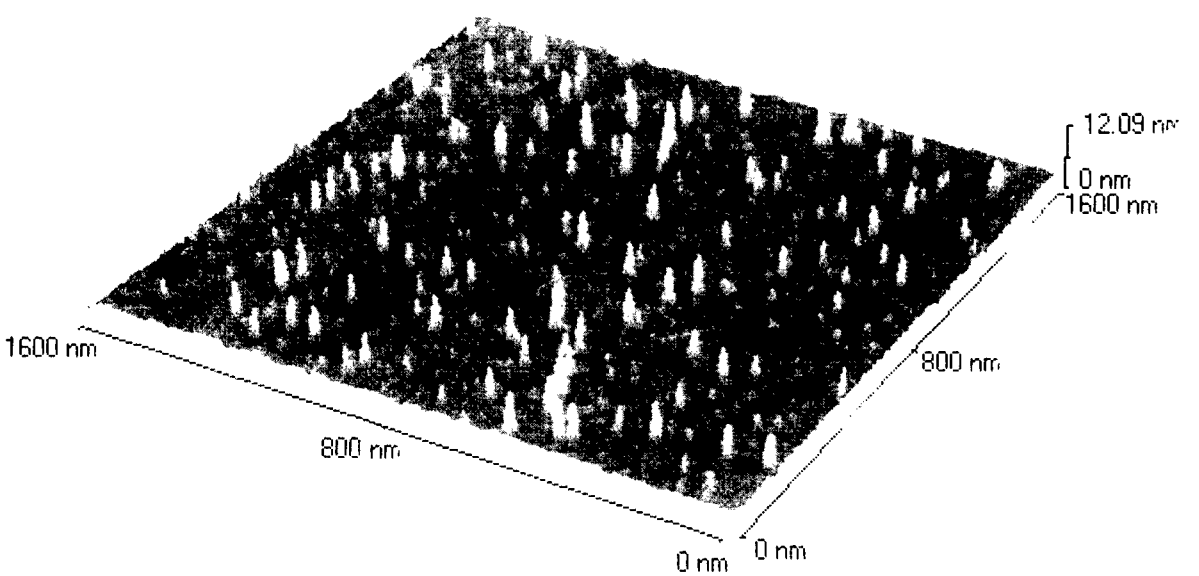

Fig. 1. Atomic force micrograph from the surface of three monolayers of InP deposited onto a GaInP buffer layer on GaAs substrate. The InP forms extremely small islands.

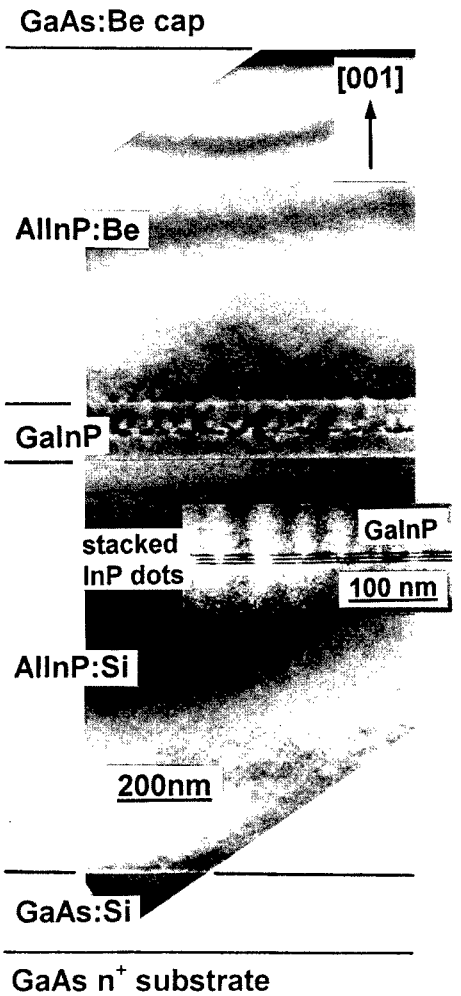

Fig. 2. Overview cross-sectional TEM micrograph of a InP quantum dot laser structure containing a 3-fold stack of InP dots embedded in the GaInP wave guide layer. The wave guide is surrounded by doped $Al_{0.53}In_{0.47}P$ cladding layers.

contrast. The 0.9 μm thick p- and n-type doped AlInP cladding layers are surrounding the $Ga_{0.52}In_{0.48}P$ wave guide layer which contains the 3-fold stack of InP dots [1,9]. Under pulsed operation we obtain the typical output power versus injection current density characteristic at 150 K which is shown in Fig. 3. Thereby the threshold current density is 265 A/cm^2. The inset shows the electroluminescence (EL) spectrum below threshold multiplied by 250. The energy position is at 1.741 eV with a FWHM of 23 meV which is in good agreement with PL measurements at 150 K (not shown here). The spectrum above threshold demonstrates a typical narrowed laser line at 1.748 eV indicating ground state QD lasing, since excited states and wetting layer luminescence is observed at higher energies of 1.80 and 1.89 eV, respectively.

Fig. 4 presents the temperature dependence of the threshold current density of three QD laser diodes with different dot sizes. With increasing dot size from nominally deposited 2.8–3.2 ML InP we obtain decreasing threshold current densities, as expected for the stronger energetic confinement of larger dots in GaInP barriers. For the sample with 3.2 ML InP dots we found a temperature independent threshold below 120 K as predicted for quantum dot lasers [3]. Above 120 K an increase is found due to thermal activated carrier evaporation out of the dots into barrier states. To achieve lasing at higher temperatures the carrier confinement has to be increased on the one hand by larger dots and on the other hand by higher barriers. The dot size reaches a limit at 3.2 ML InP due to nucleation of dislocations in the case of a stack of three or more dot layers. Thus, the more promising way is to use higher barriers, e.g. the quarternary AlGaInP or alternatively quasi-quarternary short-period superlattices (qqSL). First results from InP quantum dots in AlGaInP are presented in Ref. [10]. PL measurements on samples containing a 3-fold InP dot stack and qqSL as barriers showed one order of magnitude improvement in PL intensity at room temperature with respect to test-samples with GaInP barriers [11].

3. Atomic layer precise etching in MBE

Recently, intensity oscillations in reflection high energy electron diffraction (RHEED) have been observed during in-situ etching of GaAs using iodine [13,14], $AsCl_3$ [15–18], $AsBr_3$ [19–21] and tris-dimethylaminoarsenic (TDMAAs) [22–27]. PCl_3 was used by Tsang et al. [28] and Gentner et al. [29] for the etching of InP in CBE. The in-situ etching under optimized conditions occurs via a layer-by-layer mechanism analogous to the reverse process of MBE growth and thus provides control on the atomic scale. The combination of in-situ etching and MBE-

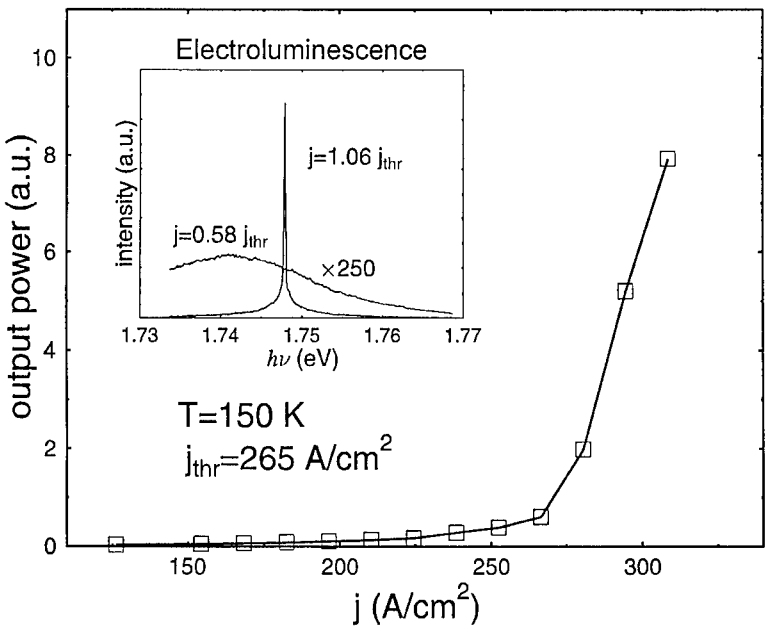

Fig. 3. Output power of the InP quantum dot laser diode versus injection current density under pulsed conditions at 150 K. The inset shows EL spectra below and above threshold current density $j_{thr} = 265$ A/cm^2 at 150 K.

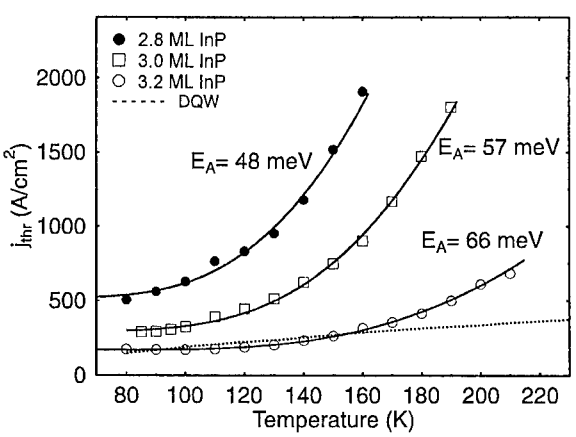

Fig. 4. Threshold current density j_{thr} versus temperature T for dot laser samples A (2.8 ML InP dots), B (3.0 ML), and C (3.2 ML) and for a GaInP/AlGaInP double quantum well laser diode as.

growth within the same MBE chamber offers considerable potential for fabricating low dimensional structures and novel devices.

We use $AsBr_3$ for the etching within a solid source MBE growth chamber, because the Br has a lower electron affinity than F and Cl and therefore less chemical reactivity against MBE equipment. $AsBr_3$ provides also arsenic over-pressure which helps to stabilize the GaAs surface even without additional As flux from a separate As source. It is available in high purity (6 N) and requires no precracking and no carrier gas. $AsBr_3$ is less critical to handle, since the melting point ($T_m = 32.8$°C) is above room temperature and the source material is kept below the melting point during etching.

In the following we describe the etching process and report selective in-situ etching of SiO_2 masked GaAs (100) substrates and MBE regrowth. Optimum conditions for thick layer GaAs etching and etching rates for GaAs/AlGaAs heterostructures and substrate orientations as a function of substrate temperature have been reported earlier [20,30].

The experiments are carried out in a modified conventional solid source MBE system with a gas manifold for $AsBr_3$ (6 N) to be introduced without carrier gas. A schematic illustration of the system set-up and a detailed description of the etching conditions are provided in Ref. [20]. Fig. 5 illustrates the etching mechanism. $AsBr_3$ molecules impinge on the surface with a beam equivalent pressure of about 2×10^{-6} mbar for a typical GaAs etching rate of 0.1 nm/s. After surface migration of adsorbed $AsBr_x$

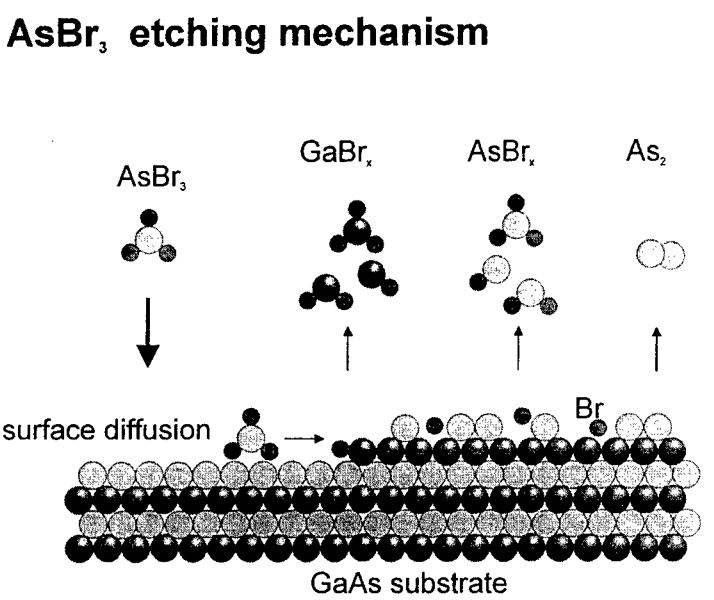

Fig. 5. Schematic illustration of the $AsBr_3$ etching mechanism of the GaAs surface.

and/or Br_x molecules $GaBr_x$ molecules are formed due to their higher binding energy compared to $AsBr_x$. The etching process is performed by $GaBr_x$ desorption from the GaAs surface. Some $AsBr_x$ molecules as well as excess As may also be desorbed. Zhang et al. [31] studied the reaction mechanism by modulated beam mass spectroscopy and found that GaBr is the main etching product. Their results indicate, that the etching rate limiting step is the formation or desorption of GaBr and not the decomposition of $AsBr_3$. Significant undercut of the SiO_2 mask in selective etching experiments discussed later in Fig. 7 indicate that surface migration of $AsBr_x$ and/or Br_x molecules is in the order of several 100 nm at temperatures above 600°C.

Fig. 6 shows RHEED intensity oscillations during GaAs growth and etching. Within the time range marked as '$AsBr_3$ etching' $AsBr_3$ molecules are supplied in addition to the Ga and As_4 fluxes for GaAs growth. That means, growth and etching are performed at the same time such that the net growth rate is reduced from about 0.7 monolayers (ML)/s to about 0.47 ML/s as indicated in the power spectrum shown in the inset of Fig. 6. The well separated sharp peaks for growth and growth plus etching indicate fast switching and quite constant etching rate within a few seconds after the $AsBr_3$ flux is

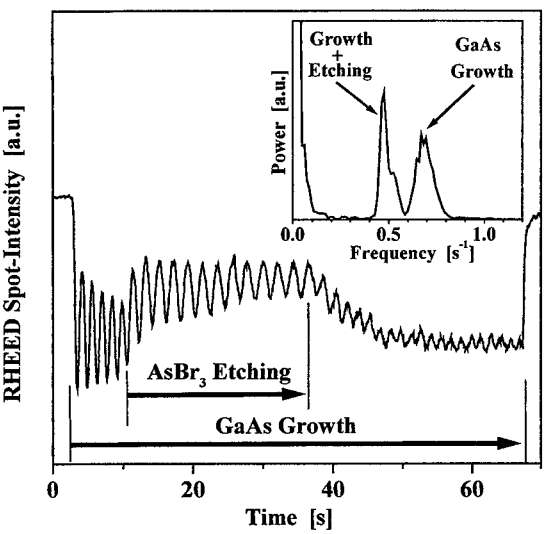

Fig. 6. RHEED intensity oscillations during growth and etching of GaAs (100). The substrate temperature was T_s = 600°C. During the period where $AsBr_3$ molecules are supplied in addition to the Ga and As_4 flux the growth rate is reduced as shown by the extended periodicity. This is quantitatively depicted in the Fourier transform spectra in the inset. The well separated sharp peaks for growth and growth plus etching indicate fast switching and constant etching as soon as the $AsBr_3$ flux is initiated and terminated.

initiated. The results in Fig. 6 together with earlier RHEED studies presented in Ref. [21] demonstrate the possibility of this technique to switch between growth and etching and vice versa within seconds. The continuous reduction of the period length after the region from growth plus etching to nominally pure growth in Fig. 6 indicates that it takes about 5–10 s before the etching is reduced down to detectable limits. It turns out that it takes a few seconds to pump away all the $AsBr_3$ which is left in the injector and the chamber to finally stop the etching process.

A possible application of this etching technique combined with epitaxial growth is to use the pronounced anisotropy of the process for in-situ surface patterning. Gentner et al. demonstrated the successful preparation of buried layer laser diodes applying PCl_3 etching and epitaxial regrowth [29]. The combination of planar facet etching and regrowth in a clean environment may also allow to realize quantum wires with improved width fluctuations by regrowth into sharp V-grooves. Fig. 7 shows a schematic illustration and scanning electron microscopy (SEM) images of selective etching of SiO_2 stripe masked GaAs (100) substrates. The stripes are oriented in the [010] direction. At low temperatures

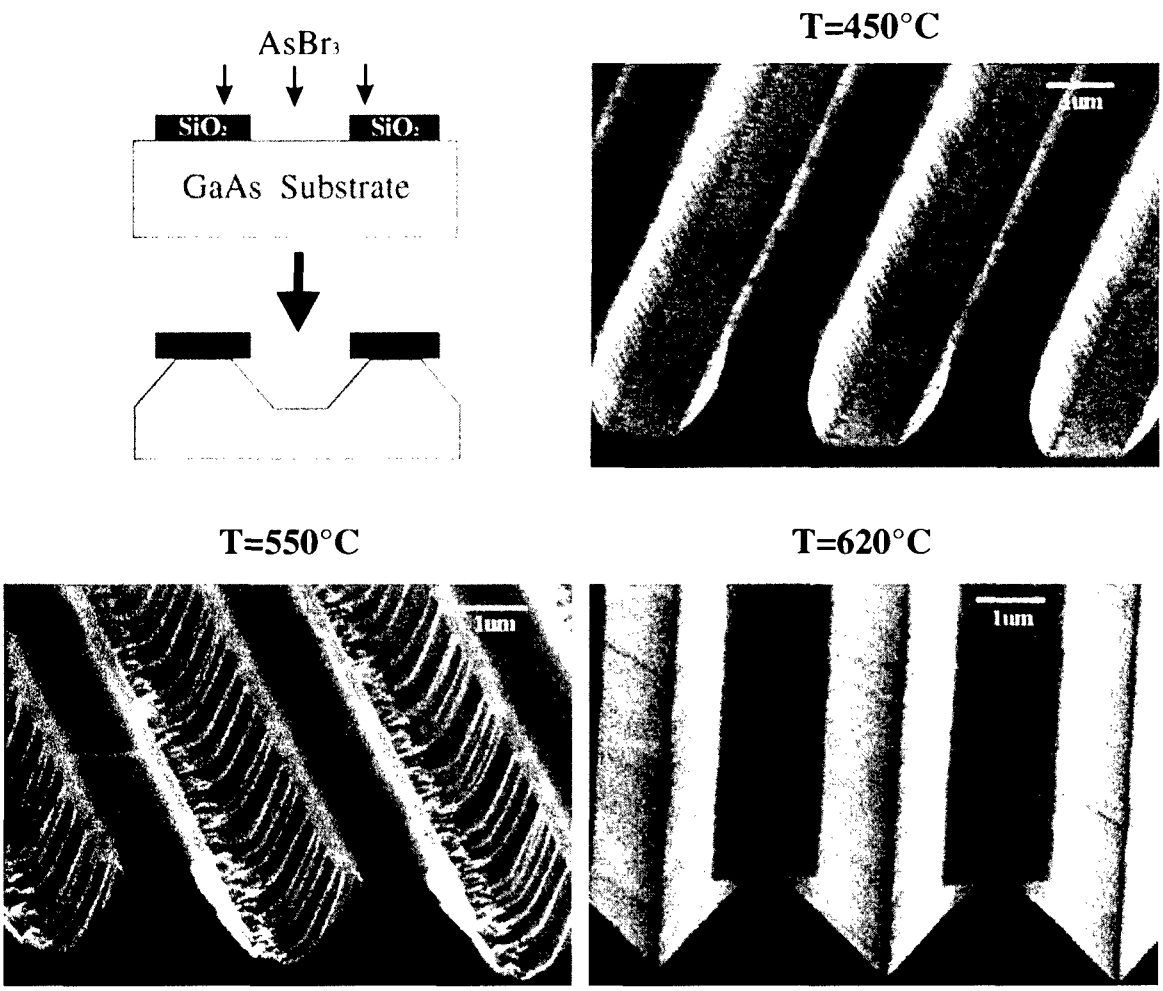

Fig. 7. Schematic illustration and SEM images of selective etching of SiO_2 stripe masked GaAs (100) substrate at different substrate temperatures. The stripes are oriented in the [010] direction. At $T_s = 620°C$ very flat {110} side facets with a sharp V-groove are produced.

of $T_s = 450°C$ there is hardly any under-etching of the SiO_2 mask and the sidewalls are {010} facets in the upper area. Towards the flat (100) bottom still relatively steep higher index facets appear. The etching depth is about 1 μm in all cases shown in Fig. 7. For $T_s = 550°C$ a clear undercut of the SiO_2 mask is observable and the shape of the groove develops already a rough V-like shape. At $T_s = 620°C$ very flat {110} 45° side facets and a sharp V-groove is achieved. The increased diffusion length of $AsBr_x$ and/or Br_x molecules causes enhanced under-etching of the mask. The GaAs edge underneath the SiO_2 mask is very sharp which is clearly seen after removing the SiO_2 mask. This is not the case for $T_s = 550°C$.

For higher substrate temperatures the {110} planes are obviously almost perfectly planarized during the etching process. The {110} planes etch slower than the other facets. This is also observed for SiO_2 mask orientation along the [01-1] direction where we observe very flat 90° facets which are again {110} planes [32].

4. Conclusions

It was demonstrated that island formation in strained layer heteroepitaxy allows the preparation of 10 nm size lateral structures without lithography in MBE. This concept is applied for quantum dot laser diodes. Lasing of a 3-fold InP dot stack within a GaInP/AlInP separate confinement heterostructure laser diode grown on GaAs substrate is observed up to $-30°C$. Significant improvement of the PL linewidth and intensity is expected after systematic optimization of growth conditions.

We demonstrated that atomic layer precise etching in solid source MBE with $AsBr_3$ is a useful technique for in-situ surface patterning. Selective etching of SiO_2 masked GaAs (100) substrates with the stripes aligned along the [100] direction provides very sharp V-grooves with almost perfectly planar {110} facets. MBE regrowth of in-situ prepared V-grooves allows the preparation of buried layers and/or completely embedded quantum wires.

The results demonstrate that the $AsBr_3$ etching is compatible with MBE growth. The switching between growth, etching and regrowth is possible within seconds. Three years experience with in-situ etching in our system did not cause any degeneracy of the sample quality. It is a clean process and does not introduce non-radiative recombination centers into the layers even when the etching step is introduced directly within the active layer of the sample.

Acknowledgements

It is a pleasure to thank W. Winter and C. Lange for excellent technical assistance and for providing the SEM and AFM images. We gratefully thank K. v. Klitzing for the continuous interest and support. This work was financially supported by the German Ministry of Education and Research (BMBF project: FKZ 01BM618/2).

References

[1] M.K. Zundel, P. Specht, N.Y. Jin-Phillipp, F. Phillipp, K. Eberl, Appl. Phys. Lett. 71 (1997) 2972, and references 1–15 therein.
[2] J.M. Gérard, O. Cabrol, B. Sermage, Appl. Phys. Lett. 68 (1996) 3123.
[3] Y. Arakawa, H. Sakaki, Appl. Phys. Lett. 40 (1982) 939.
[4] M. Asada, Y. Miyamoto, Y. Suematsu, IEEE J. Quantum Electron. 22 (1986) 1915.
[5] D. Bimberg, N. Ledentsov, M. Grundmann, N. Kirstaedter, O.G. Schmidt, M.H. Mao, V. Ustinov, A. Egorov, A. Zhukov, P. Kopev, Z. Alferov, S.S. Ruvimov, U. Gösele, J. Heydenreich, Jpn. J. Appl. Phys. 35 (1996) 1311.
[6] K. Kamath, P. Bhattacharya, T. Sosnowski, T. Norris, J. Phillips, Electron Lett. 32 (1996) 1374.
[7] H. Saito, K. Nishi, I. Ogura, S. Sugou, Y. Sugimoto, Appl. Phys. Lett. 69 (1996) 3140.
[8] S. Fafard, K. Hinzer, S. Raymond, M. Dion, J. McCaffrey, Y. Feng, S. Charbonneau, Science 274 (1996) 1350.
[9] M.K. Zundel, K. Eberl, N.Y. Jin-Phillipp, F. Phillipp, T. Riedl, E. Fehrenbacher, A. Hangleiter, Appl. Phys. Lett. 73, 28. Sept. (1998), to be published
[10] Y. Kaneko, K. Kishino, J. Appl. Phys. 76 (1994) 1809–1818.
[11] M.K. Zundel et al., in: Proc. ICPS 24th Jerusalem 1998, to be published.
[12] A. Kurtenbach, K. Eberl, T. Shitara, Appl. Phys. Lett. 66 (1995) 361.
[13] M. Micovic, C.D. Nordquist, D. Lubyshev, T.S. Mayer, D.L. Miller, R.W. Streater, A.J. SpringThorpe, J. Vac. Sci. Technol. B 16 (1998) 962.
[14] M. Micovic, D.L. Miller, F. Flack, R.W. Streater, A.J. Spring Thorpe, Appl. Phys. Lett. 69 (1996) 2680.

[15] H. Chiu, M.O. Williams, J.F. Ferguson, W.T. Tsang, R.M. Kapre, Appl. Phys. Lett. 65 (1993) 448.
[16] T. Tsang, R. Kapre, P.F. Sciortino Jr., Appl. Phys. Lett. 62 (1993) 2084.
[17] W.T. Tsang, in: K. Eberl et al. (Ed.), Low Dimensional Structures Prepared by Epitaxial Growth or Regrowth on Patterned Substrate, Vol. 298, Kluwer Academic Publishers, 1995, p. 357.
[18] J.M. Ortion, Y. Cordier, J.Ch. Garcia, C. Grattepain, J. Cryst. Growth 164 (1996) 97.
[19] K.P. Smilauer, B.A. Joyce, T. Kawamura, D.D. Vvedensky et al., Phys. Rev. Lett. 74 (1995) 3298.
[20] T. Kaneko, T. Saeger, K. Eberl, in: S.M. Prokes, R.C. Cammarata, K.L. Wang, A. Christou (Eds.), Surface/Interface and Stress Effects in Electronic Material Nanostructures, Vol. 405, Material Research Society, Pittsburgh, PA, USA, 1996, p. 67.
[21] K. Eberl, T. Kaneko, S. Maier, Electrochem. Soc. Proc. 97–21 (1997) 259.
[22] H. Asahi, X.F. Liu, K. Inoue, D. Marx, K. Asami, M. Miki, S. Gonda, J. Cryst. Growth 145 (1994) 668.
[23] T. Hayashi, H. Asahi, K. Yamamoto, K. Hidaka, S. Gonda, Jpn. J. Appl. Phys. 35 (1) (1996) 3814.
[24] C.W. Tu, N.Y. Li, Electrochem. Soc. Proc. 97–21 (1997) 10.
[25] N.Y. Li, C.W. Tu, Compound Semiconductor Electronics and Photonic, Mater. Res. Soc. Symp. Proc. 421 (1996) 15.
[26] N.Y. Li, Y.M. Hsin, W.G. Bi, P.M. Asbeck, C.W. Tu, Appl. Phys. Lett. 70 (1997) 2589.
[27] J. Sato, H. Asahi, T. Tashima, K. Hidaka, K. Yamamoto, K. Asami, S. Gonda, J. Cryst. Growth 188 (1998) 363.
[28] W.T. Tsang, T.H. Chiu, R.M. Kapre, Appl. Phys. Lett. 63 (1993) 3500.
[29] J.L. Gentner, P. Jarry, L. Goldstein, IEEE J Select. Top. Quantum Electronics 3 (1997) 845.
[30] M. Ritz, T. Kaneko, K. Eberl, Appl. Phys. Lett. 71 (1997) 695.
[31] J. Zhang, O.P. Naji, P. Steans, P. Tejedor, T. Kaneko, T.S. Jones, B.A. Joyce, J. Cryst. Growth 175/176 (1997) 1284.
[32] H. Schuler, M.O. Lipinski, K. Eberl, Semicond. Sci. Technol. 15 (2000) 169.